

A Hierarchical Model Predictive Servo Control Framework Based on Dynamic Matrix Control for High-Performance PMSM Position Tracking Systems

Yimeng Wen
Yangtze University
College of Education and Sports Science
Jinzhou, China

Abstract: High-performance permanent magnet synchronous motor (PMSM) servo systems are widely adopted in precision motion control applications; however, conventional cascaded PI/PID architectures suffer from performance degradation under large reference transients, parameter uncertainties, and actuator saturation constraints. These limitations often manifest as overshoot, prolonged settling time, and integral windup, which significantly restrict the achievable dynamic performance and robustness of industrial servo drives.

To address these challenges, this paper proposes a hierarchical model predictive control (MPC)-inspired servo framework based on Dynamic Matrix Control (DMC) for PMSM position tracking systems. The proposed approach establishes a reduced-order discrete-time predictive model derived from the step-response representation of the speed subsystem, enabling computationally efficient non-parametric prediction without requiring explicit full-state system identification. On this basis, a three-layer cascaded control architecture is developed, consisting of an outer-loop proportional-derivative (PD) position controller, a middle-layer DMC-based velocity predictive optimizer, and an inner-loop current regulation stage.

To further enhance practical applicability, multi-rate sampling coordination is introduced to decouple electrical and mechanical dynamics, allowing high-frequency current regulation and low-frequency predictive optimization to coexist within a unified control framework. In addition, explicit hard constraints on current magnitude and variation rate are embedded into the DMC optimization problem, together with an anti-windup feedback correction mechanism to mitigate performance degradation under actuator saturation. A reference trajectory smoothing strategy is also incorporated to improve transient behavior and suppress aggressive control actions.

Simulation results based on MATLAB/Simulink demonstrate that the proposed method achieves zero-overshoot position tracking, significantly reduced settling time, and enhanced disturbance rejection capability compared with conventional cascaded PI control schemes. Moreover, under sudden load disturbances, the proposed controller exhibits superior dynamic stiffness and faster recovery performance while maintaining bounded current profiles and improved electrical safety. These results validate the effectiveness of the proposed DMC-based hierarchical control framework for high-performance PMSM servo applications with stringent real-time and constraint requirements.

Keywords: Permanent Magnet Synchronous Motor (PMSM); Dynamic Matrix Control (DMC); Model Predictive Control (MPC); Cascaded Control System; Servo Position Tracking; Constraint Handling; Anti-windup; Multi-rate Sampling

1. INTRODUCTION

Permanent Magnet Synchronous Motors (PMSMs) have become the core actuating units in high-precision servo drive systems due to their high power density and excellent dynamic performance. Most existing industrial systems adopt a cascaded three-loop architecture consisting of position, speed, and current control. However, conventional linear feedback controllers such as PI/PID increasingly reveal performance limitations under complex operating conditions. These limitations are mainly reflected in insufficient robustness against system nonlinearities, parameter variations, and external disturbances. Moreover, under actuator saturation constraints, such controllers are prone to integral windup and dynamic oscillations, which ultimately restrict the achievable trade-off among response speed, tracking accuracy, and robustness.

To overcome these limitations, advanced control strategies such as sliding mode control, adaptive control, and intelligent control have been proposed, which improve disturbance rejection capability to some extent. Nevertheless, these approaches often suffer from implementation complexity, chattering phenomena, and difficulties in stability analysis, leading to significant engineering constraints in practical applications. In recent years, Model Predictive Control (MPC) has emerged as a promising direction in servo drive systems

due to its multi-step prediction capability and explicit constraint handling. Among its variants, Dynamic Matrix Control (DMC) performs rolling optimization based on step-response modeling and has been successfully applied to motor drive systems with the advancement of embedded computing capabilities. It enables effective handling of constraints such as current, voltage, and duty cycle, thereby improving dynamic performance under extreme operating conditions.

However, in high-frequency PWM-based servo systems, predictive control still faces several critical challenges, including model accuracy, the computational complexity of online optimization, and multi-rate sampling coordination. In particular, for systems with pronounced integral characteristics in the position loop, direct full-scale predictive control may lead to excessively high computational dimensionality and compromised real-time performance. Consequently, recent research has increasingly focused on hierarchical cascaded architectures that combine inner-loop predictive optimization with simplified outer-loop control, aiming to achieve high-performance position tracking under complex constraints while maintaining both dynamic performance and engineering feasibility.

2. Selection and Principles of Control Methods

2.1 Mathematical Models and Control Methods

As a core actuator in servo positioning systems, the Permanent Magnet Synchronous Motor (PMSM) requires an accurate mathematical model to support the design of Dynamic Matrix Control (DMC) algorithms and to analyze the characteristics of the controlled plant. Figure 1 illustrates the physical structure of the PMSM and the definition of its spatial coordinate system.

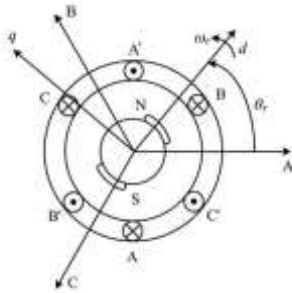


Figure 1 Schematic diagram of the physical structure and spatial coordinate system of the Permanent Magnet Synchronous Motor

When constructing the spatial coordinate reference frame, the A-phase stator winding axis is selected as the reference axis of the stationary coordinate system. The direction of the magnetomotive force generated by each phase winding under positive conduction current is defined as the positive direction of its respective reference axis. According to the law of electromagnetic induction, the positive direction of the induced electromotive force in the stator windings is defined as opposite to the direction of the current. Meanwhile, the counterclockwise rotation of the rotor is uniformly defined as the positive direction for mechanical speed and electromagnetic torque.

2.1.1 Modeling premises and idealized assumptions

Due to the inherently multivariable, strongly coupled, nonlinear, and high-order time-varying nature of the Permanent Magnet Synchronous Motor (PMSM), direct analysis based on its original physical model makes it difficult to extract the linear response matrices (e.g., step or impulse response sequences) required for the multi-step prediction in Dynamic Matrix Control (DMC). Therefore, in order to overcome the computational bottleneck of conventional nonlinear modeling in practical implementations of predictive control algorithms, and to facilitate system simplification and coordinate decoupling, the following idealized assumptions are introduced prior to model derivation:

- (1) The magnetic saturation of the stator core is neglected, assuming a linear magnetic circuit, while hysteresis and eddy current losses are ignored;
- (2) The damping effect of the rotor is neglected, i.e., no damper windings are considered and the permanent magnets are assumed to be free of damping effects;
- (3) The three-phase stator windings are assumed to be perfectly symmetrical and uniformly distributed in the stator slots, with spatial displacement of 120 electrical degrees between phases;
- (4) The air-gap magnetic field is assumed to be ideally sinusoidal, and both the induced electromotive force and

magnetomotive force are considered pure sinusoidal waveforms, neglecting the influence of spatial harmonic components on electromagnetic torque.

Based on the above assumptions, the voltage and flux linkage vector equations of the stator three-phase system in the three-phase stationary reference frame (ABC frame) can be further expressed as follows:

$$i_s = \sqrt{\frac{2}{3}} (i_A + ai_B + a^2i_C)$$

In the formula, i_A , i_B and i_C are the three-phase stator currents, respectively; a is the space operator, $a=ej120^\circ$.

Then the stator voltage equation is:

$$u_s = R_s i_s + L_s \frac{di_s}{dt} (\psi_f e^{j\theta_r})$$

In the formula, u_s is the stator voltage space vector; R_s is the stator phase resistance; and L_s is the stator equivalent synchronous inductance.

2.2 Discretization modeling

2.2.1 Velocity loop equivalent continuous transfer function

In a speed-current cascaded control system for a permanent magnet synchronous motor, the bottom current loop typically employs a PI controller combined with SVPWM modulation technology. Because the electrical time constant of the current loop is extremely small, and its system bandwidth is much higher than that of the mechanical speed loop, its closed-loop gain in the low-frequency range is approximately 1. Therefore, assuming the current loop responds extremely quickly and stably, the slight high-frequency hysteresis effect of the inner current loop can be ignored.

Based on this equivalence, the dynamic process of the controlled object from the quadrature-axis current command i_q^* (input) to the motor's mechanical speed n (output) is mainly constrained by mechanical parameters such as the rotor's moment of inertia and viscous friction coefficient. This dynamic process can be reduced in order and approximately equivalent to a typical first-order inertial element, whose continuous transfer function $G(s)$ can be expressed as:

$$G(s) = \frac{n(s)}{i_q^*(s)} = \frac{K_{plant}}{T_{plant}s + 1}$$

K_{plant} is the equivalent static gain of the velocity loop;

T_{plant} is the equivalent mechanical time constant .

2.2.2 Discretization and step response extraction of the prediction model

Dynamic Matrix Control (DMC), as an advanced computer numerical control algorithm, relies on multi-step prediction and rolling optimization using the discrete step response of the controlled object. Therefore, the continuous first-order model $G(s)$ needs to be discretized within the sampling period T_s of the control system (set to 1 ms in this paper).

By introducing a zero-order hold (ZOH), the continuous first-order inertial element can be transformed into a corresponding difference equation. Let $u(k)$ be the quadrature-axis current command at the k -th step, and $n(k)$ be the speed feedback value at the k -th step. The expression for the discretized speed loop difference equation is as follows:

$$n(k+1) = a \cdot n(k) + (1-a) \cdot K_{plant} \cdot u(k)$$

In the formula, coefficient 'a' is the inertial decay factor after system discretization, which is determined by the sampling period T_s and the system time constant T_{plant} .

The prediction model of the DMC algorithm does not rely on the precise parameterized state equation, but is based on the system's true discrete step response sequence. Based on the above difference equation, let the initial state $n(0)=0$, apply a unit step signal (i.e., $u(k)=1$), and the step response coefficient sequence of the system in the future finite time domain can be obtained through recursive iteration:

$$g_i = a \cdot g_{i-1} + (1-a) \cdot K_{plant} \quad (i = 1, 2, \dots, N)$$

In the formula, N represents the modeling time domain of the DMC algorithm. This step response coefficient sequence fully encompasses the dynamic evolution law of the controlled motor under step commands. It is the basis for constructing the "dynamic matrix" of the control system and the core mathematical basis for DMC rolling optimization and

feedback correction in Chapter 3.

3. Dual Closed-Loop Controller Design

3.1 Design of Outer Loop Position Controller

In the cascaded dual-loop architecture designed in this paper, the main task of the outer-loop position controller is to eliminate the system's position tracking error and provide a smooth and reasonable target speed command for the inner dynamic matrix controller (DMC). To balance the system's fast response and anti-interference capability, this paper designs an improved proportional-derivative (PD) controller with speed feedforward compensation.

3.1.1 Design of an improved PD control law with velocity feedforward

Traditional position control typically employs a classic PID controller. However, in servo positioning, the target position command often exhibits a step change. If the position deviation is directly differentiated, the abrupt change in deviation at the step will cause the differential term to output a pulse signal approaching infinity, a phenomenon commonly known in industrial control as the "derivative kick." This phenomenon can cause severe oscillations in the motor current, significantly affecting the system's stability.

To avoid this problem, this paper adopts an improved "derivative-first" PD control law. Considering that in actual servo motors, the derivative of the rotor mechanical angle is the actual rotor speed, and the physical speed cannot change abruptly due to mechanical inertia, the actually measured speed is directly introduced as the differential term feedback. The mathematical expression of its discrete control law is as follows:

$$\omega_{ref}(k) = K_p [\theta_{ref}(k) - \theta_m(k)] - K_d \omega_m(k)$$

In the formula, $\omega_{ref}(k)$ represents the target rotational speed command output in the k -th cycle; $\theta_{ref}(k)$ and $\theta_m(k)$ represent the target position and the actual feedback position, respectively; K_p is the proportional gain; and K_d is the differential gain. This structure ensures rapid proportional amplification of position deviations while utilizing the actual rotational speed to construct negative feedback damping, effectively suppressing the overshoot tendency of the system when approaching the target position.

3.1.2 Position loop output constraint and limiting processing

The target speed command calculated by the PD control law is directly fed into the inner DMC speed controller as a reference trajectory. However, in practical engineering applications, the motor's maximum speed is limited by the inverter's DC bus voltage and back EMF; simultaneously, excessively large command mutations can significantly increase the prediction error of the DMC algorithm during rolling optimization, leading to severe overshooting and impacts in the quadrature-axis current calculated by the inner layer.

Therefore, strict hard constraints must be applied to the position loop output. Specifically, this includes two dimensions of limiting:

1. Amplitude limiting (absolute speed saturation): Limiting ω_{ref} the speed command within the safe range allowed by the motor's rated speed to prevent it from exceeding the physical boundaries of the underlying layer.
2. Rate of change limiting (acceleration saturation): Limiting the increment of the speed command between $[-\omega_{max}, \omega_{max}]$ two adjacent control cycles.

Through this dual limiting process, not only is the safety of the motor and power electronic hardware ensured, but a smooth, physically attainable desired trajectory is also provided for the inner-loop DMC algorithm, thereby significantly improving the overall robustness and dynamic solution quality of the cascaded predictive control system.

3.2 Design of Speed Loop Dynamic Matrix Controller (DMC)

In the cascaded control architecture designed in this paper, the speed inner loop is the core factor determining the dynamic response quality of the system. To overcome the problems of overshoot and excessively long settling time that traditional PI controllers are prone to when facing nonlinear friction of motors and sudden loads, this paper introduces a dynamic matrix control (DMC) algorithm into the speed loop. The DMC algorithm achieves highly dynamic, overshoot-free, and accurate tracking of the target speed command through nonparametric model prediction, reference trajectory softening, rolling optimization solution, and closed-loop feedback correction.

3.2.1 Construction of non-parametric prediction models

The DMC algorithm breaks away from the traditional control's reliance on precise state spaces or differential equations, directly using the unit step response sequence of the controlled object as a non-parametric prediction model. Continuing from the velocity loop equivalent discrete model

extracted above, let its response coefficient sequence under a unit step input be g_1, g_2, \dots, g_N (N is the modeling time domain).

Assuming that at the current time k , the future control increment sequence of the system is $\Delta u(k), \dots, \Delta u(k+M-1)$ (where M is the control time domain), then the predicted output vector of the system in the next P steps (P is the prediction time domain, $M \leq P \leq N$) can be obtained by adding the system's free response vector to the forced response, and its matrix expression is:

$$Y_p = Y_{p0} + A\Delta U$$

, $\Delta U = [\Delta u(k), \Delta u(k+1), \dots, \Delta u(k+M-1)]^T$ is the control increment vector; Y_{p0} is the system free prediction output vector when all future control increments are assumed to be zero; A is a dimensional dynamic matrix composed of step response coefficients, which reflects the dynamic influence of the control action on the future output of the system.

3.2.2 Reference trajectory softening and scrolling optimization

(1) Reference Trajectory Softening

During servo positioning, the target speed command output by the outer loop PD controller may have a step jump. To avoid excessively large transient errors causing overly drastic control action, the DMC algorithm uses a first-order exponential filtering formula to generate a smooth reference trajectory:

$$y_r(k+i) = \alpha^i y(k) + (1-\alpha^i) y_{ref}(k) \quad (i = 1, 2, \dots, P)$$

In the formula, $y(k)$ is the actual rotational speed feedback value at the current moment; $y_{ref}(k)$ is the set target rotational speed; and α is the smoothing coefficient ($0 < \alpha < 1$). The larger α is, the smoother the process of the reference trajectory approaching the target value, and the stronger the robustness of the system; conversely, the response is faster but it is prone to overshoot.

(2) Rolling Optimization Solution

The goal of the DMC algorithm is to make the predicted output as close as possible to the reference trajectory over the next P time steps, while avoiding drastic changes in the control input. To this end, a quadratic objective function J is constructed, which includes error penalty and control increment penalty:

$$J = \sum_{i=1}^P q_i [y_r(k+i) - \hat{y}(k+i|k)]^2 + \sum_{j=1}^M r_j [\Delta u(k+j-1)]^2$$

Convert it to matrix-vector form as follows: $J = \| Y_R - Y_p \|_Q^2 + \| \Delta U \|_R^2$

In the formula, Q is the error weight matrix, and R is the control increment weight matrix. Substituting the prediction model $Y_p = Y_{p0} + A\Delta U$ into the objective function and

letting $\frac{\partial J}{\partial \Delta U} = 0$, the optimal control increment

analytical solution under unconstrained conditions can be obtained using the least squares method:

$$\Delta U = (A^T Q A + R)^{-1} A^T Q (Y_R - Y_{p0})$$

In the actual rolling optimization mechanism, only the first element ΔU of the vector $\Delta u(k)$ is applied to the system each time, and the prediction and solution are re-performed using the new measurement value at the next time step.

3.2.3 Error feedback correction and improved hard constraint processing

(1) Error Feedback Correction

Due to perturbations in internal motor parameters or external load torque disturbances, deviations inevitably exist between the output of the prediction model and the actual output. Before each step of the calculation, the DMC algorithm calculates the prediction error using the actual measured speed at the current moment and the predicted value at the previous moment. Then, it uses the error correction vector to compensate for the shift in the future free response, thereby endowing the controller with strong anti-interference and closed-loop robustness.

(2) Hard Constraint Limiting and Anti-Integral Saturation Mechanism

The theoretical control increment obtained based on the analytical solution corresponds, in a physical sense, to the change in the quadrature-axis current command. Traditional DMC algorithms typically assume that the actuator is ideally linear, but this is prone to failure in motor drive systems with strict physical boundaries. Therefore, this paper adds a hard constraint treatment for the quadrature-axis current at the end of the algorithm:

First, the rate of change of current is limited to prevent sudden current changes from damaging the inverter:

$$\Delta u^*(k) = \text{sat}(\Delta u(k), \Delta i_{q_{\max}})$$

Secondly, the absolute amplitude of the final output current is limited to prevent motor overload:

$$u^*(k) = \text{sat}(u(k-1) + \Delta u^*(k), i_{q_{\max}})$$

A more crucial improvement lies in the update logic of the prediction model. When a sudden change in system commands causes current hardware saturation, if the theoretically calculated, $\Delta u(k)$ excessively large value is still used to update the initial prediction value for the next cycle, the predicted trajectory within the controller will deviate significantly from the physical reality, leading to "model mismatch" and integral saturation oscillation. To address this issue, this paper reverse-engineers the actual current increment acting on the motor after limiting in the code implementation:

$$\Delta u_{\text{actual}}(k) = u^*(k) - u(k-1)$$

It also forces the use of this real data for iterative updates of the prediction model. This anti-windup improvement mechanism ensures that the internal "cognition" of the DMC controller is always highly synchronized with the physical

boundary of the motor, fundamentally eliminating the oscillation phenomenon when the system enters and exits the saturation region, and significantly improving the positioning stability of the servo system.

3.3 Vector control and PI current loop design

In the cascaded control architecture designed in this paper, the inner current loop is at the bottom layer of the system. Its core task is to quickly and accurately follow the stator current commands issued by the upper-level controller, thereby providing the motor with stable and controllable electromagnetic torque.

Continuing from the design in the previous section, the control quantity output by the Dynamic Matrix Controller (DMC) after rolling optimization and hard constraint limiting serves as the quadrature-axis current command i_q for the inner current loop. Simultaneously, based on the mathematical model of the permanent magnet synchronous motor (PMSM) described in Chapter 2, to achieve complete decoupling of the torque component and the excitation component, and to eliminate the interference of armature reaction on the air gap main magnetic field, this paper strictly adopts a vector control strategy with zero direct-axis current ($i_d=0$) at the bottom layer. This strategy ensures that the electromagnetic torque is only proportional to the quadrature-axis current, providing an ideal linearized controlled object for the upper-level DMC algorithm.

During the closed-loop control implementation, the system collects the stator three-phase current in real time through current sensors and extracts the actual feedback currents i_d and i_q in the synchronous rotating coordinate system through Clark and Park coordinate transformation. Subtracting the reference command from the actual feedback value yields the dual-axis current errors: $e_d = i_d^* - i_d$ and $e_q = i_q^* - i_q$. Since the stator electrical time constant is extremely small, and the decoupled current model approximates a first-order inertial element, excellent zero-steady-state-error tracking can be achieved independently using a traditional proportional-integral (PI) controller for both axes. The equivalent mathematical model of its current loop is shown in Figure 2.

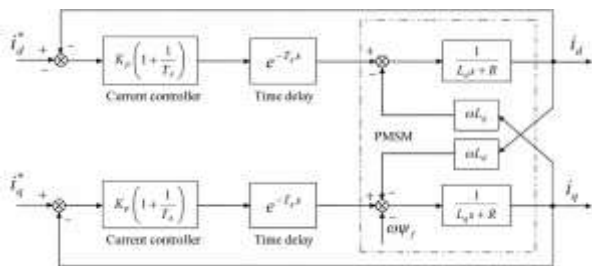


Figure 2 Equivalent mathematical model diagram of current loop

4. Simulation Results Analysis

Based on the above principles and ideas, a vector control system for a permanent magnet synchronous motor was built. A load was applied to the motor at 0.3s to test its stability under load. The given frequency of the motor was set. Simulation results were obtained, including the three-phase current of the stator, electromagnetic torque, stator flux linkage, and changes in electron speed. Finally, the simulation results were analyzed based on the waveform diagrams.

4.1 Comparative analysis of no-load position step tracking performance

To verify the basic dynamic performance of the improved DMC cascaded control system designed in this paper, a position step tracking test was first conducted under motor no-load conditions. The system was initially set to a completely stationary state, and a sudden change (from 0 rad to 10 rad) occurred when a target position command was given at time $t = 0$ s. This section will focus on observing and comparing the key dynamic indicators such as position, speed, and current of the traditional three-loop PI system and the improved system in this paper during the step response process.

4.1.1 Position tracking response comparison

Position tracking curves are the most intuitive indicator for measuring the macroscopic control quality of a servo positioning system. Actual rotor position response data under two control strategies were imported into the same coordinate system for comparison, and the results are shown in the figure 3.

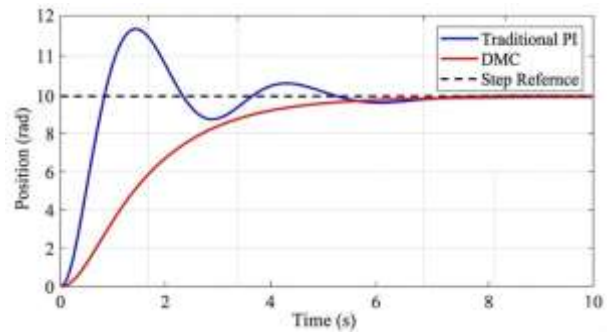


Figure 3 Comparison of no-load position step tracking response between traditional PI and improved DMC systems

As shown in Figure 21, the traditional PI control system exhibits significant overshoot (approximately 16%) when approaching the target position due to severe integral accumulation (windup) in both the outer and inner loop PI controllers when faced with large-range position step commands. This is accompanied by several damped oscillations, finally converging to a steady-state value of 10 rad after about 7 seconds.

In contrast, the "outer loop PD + inner loop DMC" system designed in this paper demonstrates a remarkably significant performance advantage. Thanks to the predictive optimization and reference trajectory softening mechanism of the DMC algorithm, the position tracking curve exhibits a smooth and strictly overshoot-free monotonically increasing characteristic, achieving ideal "zero overshoot" servo positioning. Furthermore, by completely eliminating the repeated oscillation adjustment process after exceeding the target value, the DMC system's settling time is shortened to approximately 6 seconds, significantly improving the system's rapid positioning and tracking capabilities.

4.1.2 Dynamic response analysis of internal state variables (speed and current)

The quality of a high-performance servo system is not only reflected in the final position curve, but also in the smoothness of the transition of its internal state variables (speed and current), which directly determines the mechanical life and electrical safety of the actuator.

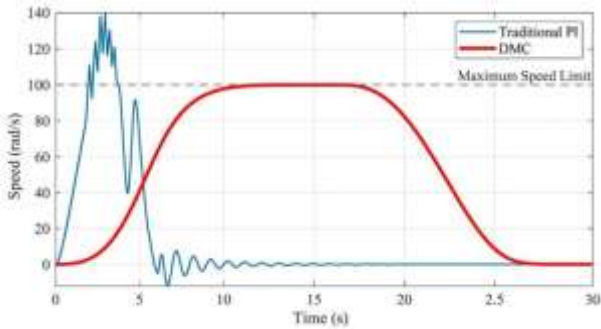


Figure 4 Comparison of speed dynamic response between traditional PI and improved DMC systems

Figure 4 shows a comparison of the dynamic response of motor speed during step tracking. In the initial startup phase, both controllers can quickly output acceleration commands. However, the speed curve of the traditional PI system exhibits significant lag and sharp fluctuations during deceleration and braking; the DMC controller in this paper strictly adheres to the maximum speed limit set internally by the algorithm (the limiting mechanism is in effect), ensuring that the speed operates within a safe range. More importantly, when approaching the target position, the DMC algorithm can "predict" future trajectory errors and smoothly reduce the target speed in advance, achieving an extremely gentle braking transition.

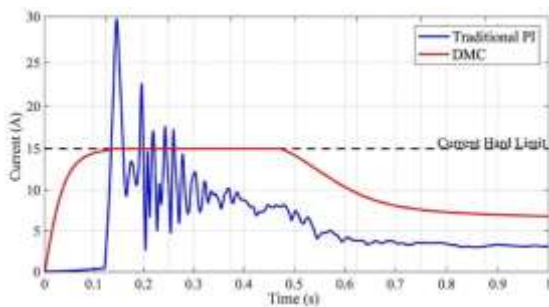


Figure 5 Comparison of start-up response of quadrature-axis current (iq) between traditional PI and improved DMC systems

The paper further illustrates the response waveform of the quadrature-axis current (i.e., equivalent electromagnetic torque) at the system's underlying layer. At the instant of a sudden position step, the speed loop of a traditional PI system is prone to outputting a huge saturation current command, generating a transient large current surge, which is extremely detrimental to the inverter's power devices. The DMC algorithm in this paper introduces a penalty weight for the control increment in the rolling optimization objective function and adds dual hard constraints on the rate of change of current and absolute amplitude. As can be clearly seen from the figure, the starting current rise of the improved system is smoother, and the transient surge peak is effectively suppressed. This demonstrates that the algorithm in this paper significantly improves the underlying electrical safety while ensuring high dynamic response.

4.2 Comparative Analysis of Immunity Performance under Sudden Loading

High-performance servo systems not only require excellent command tracking capabilities but also strong resistance to external disturbances to ensure positioning accuracy under complex operating conditions. This section aims to verify the

system's dynamic stiffness and anti-disturbance recovery capability. The motor is assumed to be running stably under no-load and stationary at the target position of 10 rad before $t=0.5s$. At $t=0.5s$, a step load torque of magnitude is suddenly applied to the motor shaft. The dynamic response processes of the two control architectures under disturbed conditions are compared and analyzed.

4.2.1 Position drop and recovery under load disturbance

The sudden intervention of external load torque will disrupt the original torque balance of the motor, causing the rotor to be dragged in the opposite direction, and the actual position will inevitably deviate from the set target. Figure shows the position tracking response curve of the system at the moment of sudden load application.

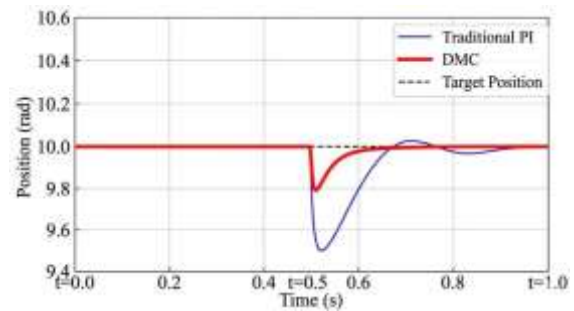


Figure 6 Dynamic waveform diagram of system position drop and recovery under sudden load disturbance

As shown in Figure, the traditional three-loop PI control system, due to the inherent phase lag of the integral element, is slow to detect and compensate for sudden disturbances, resulting in a large position drop (maximum deviation error of approximately 0.5 rad) and requiring a long adjustment period of about 0.4 s to recover to a steady state. In contrast, the improved DMC cascade system in this paper exhibits stronger "dynamic stiffness." Its position drop is significantly reduced to only 0.18 rad, and the rotor is rapidly pulled back and locked at the target position of 10 rad within 0.05 s, without any secondary oscillations. This intuitively demonstrates that the DMC algorithm has superior robustness in handling unknown external disturbances.

4.2.2 The process of adjusting speed and electromagnetic torque

To explore the underlying mechanism of the above-mentioned differences in anti-disturbance performance, the dynamic response waveforms of rotational speed and electromagnetic torque inside the system during the disturbance were further extracted, as shown in Figure 7 and Figure 8, respectively.

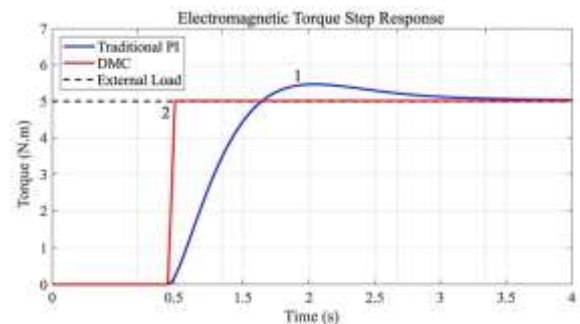


Figure 7 Waveforms of speed drop and reverse compensation of the system under sudden load disturbance.

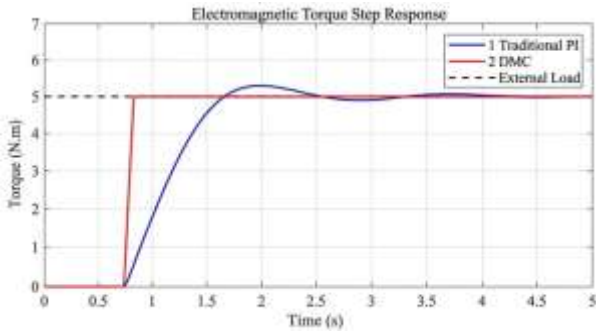


Figure 8 Comparison of electromagnetic torque step response under sudden load disturbance

As shown in Figure 7, at the instant the load is applied at $t=0.5$ s, the motors in both systems passively reverse (the speed drops below zero). However, the DMC system can output a positive compensation speed command with a more sensitive response speed, quickly compensating for the angular displacement lost due to the disturbance.

The electromagnetic torque waveform in Figure 26 reveals the advantages of the DMC algorithm from the lowest level. After a sudden load is applied, the stator must quickly output an equivalent electromagnetic torque re-establish torque balance. Traditional PI controllers rely on the slow accumulation of position and speed errors to gradually increase the current command; while the DMC algorithm has a powerful error feedback correction mechanism. Within a very short time after detecting that the actual speed deviates from the predicted trajectory, DMC immediately corrects the predicted value of the future free response using the correction vector, and quickly calculates the required optimal compensation increment in the next rolling optimization. Therefore, the electromagnetic torque of the DMC system can jump to the required steady-state value with a near-vertical slope, fundamentally curbing the further expansion of the position error with an extremely rapid underlying current response.

4.3 Analysis of the impact of DMC key parameters on control performance

The superiority of the Dynamic Matrix Control (DMC) algorithm lies not only in its ability to handle hard constraints, but also in the clear physical meaning of its key parameters, which are highly compatible with engineering tuning requirements. This section takes the reference trajectory smoothing coefficient, the most crucial parameter in the DMC algorithm, as an example to explore the specific impact of its numerical variation on the position tracking performance of the servo system, in order to verify the algorithm's adjustability and the rationality of the parameter selection presented in this paper. In the theoretical framework of DMC, the smoothing coefficient is used to construct a smooth transition trajectory that approximates the target value for the desired output. The value of directly determines the "aggressive" or "conservative" degree of the controller output. To intuitively present this effect, other control parameters (such as prediction time domain P, control time domain M, and control weight R) are kept constant, and $\alpha = 0.5$, $\alpha = 0.85$ and $\alpha = 0.95$ are set respectively. A position step tracking simulation test is performed under no-load conditions, and the comparative response curves are shown in Figure 9.

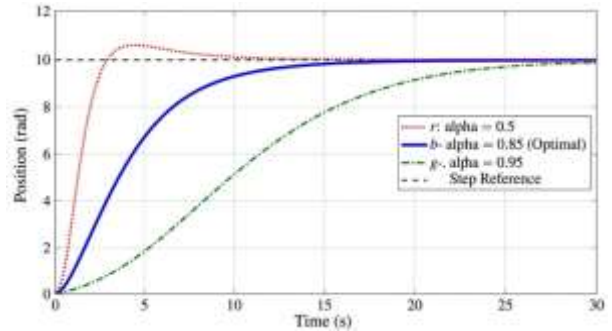


Figure 9 Comparison of position step tracking response under different softening coefficients α

Based on the waveform evolution pattern in Figure 9, the following conclusions can be drawn:

- (1) When the value of α is small (e.g. $\alpha = 0.5$), the system's reference trajectory approaches the target extremely aggressively, with a very short rise time. However, excessively rapid changes in speed commands frequently trigger the hard constraint saturation of the inner loop current, and may even induce slight high-frequency oscillations near the target position, reducing operational stability.
- (2) When the value of α is large (e.g. $\alpha = 0.95$), the reference trajectory is extremely smooth, and the control action is relatively conservative. At this time, the system operates extremely smoothly and has strong anti-disturbance robustness, but due to the excessively slow initial acceleration, the overall settling time is significantly prolonged, sacrificing the high dynamic response capability that the servo system should possess.
- (3) When the value of α is adopted as specified $\alpha = 0.85$ in this paper, the system's dynamic response achieves an excellent balance between speed and stability. The position curve can both quickly overcome the transient process and exhibit excellent smooth braking characteristics when approaching steady state, achieving true "no overshoot, fast convergence".

In summary, the tuning of the smoothing coefficient is essentially a comprehensive trade-off between system response speed and stability. The comparative test data in the preceding sections of this paper were all obtained under the optimized configuration, and the simulation results fully verify the scientific nature and optimality of the parameter selection.

5. Summary

This paper addresses the problems of significant overshoot, long settling time, insufficient disturbance rejection, and difficulty in effectively handling actuator constraints in permanent magnet synchronous motor (PMSM) servo positioning systems under large-scale step commands and complex load disturbances. Taking surface-mounted permanent magnet synchronous motors (SPMSMs) as the research object, an improved cascaded position tracking control strategy based on dynamic matrix control (DMC) is proposed. First, a nonlinear mathematical model of the motor is established based on the d-q synchronous rotating coordinate system, and an equivalent discrete model of the speed loop is derived based on $i_d=0$ vector control. The system step response sequence is extracted to construct a DMC prediction model. Second, a multi-rate cascaded control

architecture of "position PD—speed DMC—current PI" is designed. By introducing a speed loop prediction optimization mechanism, the dynamic response and trajectory tracking performance of the system are improved while reducing computational complexity. Furthermore, to address the saturation constraint problem in practical drive systems, dual constraints of current amplitude and rate of change are introduced in the DMC optimization process. An incremental feedback correction mechanism is used to suppress model mismatch and integral accumulation effects caused by saturation, thereby enhancing the stability and engineering applicability of the system under extreme conditions. Overall, this method achieves a synergistic improvement in the dynamic performance and robustness of the servo system while ensuring real-time feasibility. Fourth, it completes the simulation and multi-dimensional performance verification of the control system under multiple operating conditions. A complete motor control system model was built using the MATLAB/Simulink platform. The no-load position step simulation results show that, compared with the traditional three-closed-loop PI system, the DMC cascade system designed in this paper achieves perfect "zero overshoot" fast positioning and effectively suppresses the overload current impact at startup. The simulation with sudden rated load further proves that, thanks to the sensitive error correction mechanism of the DMC algorithm, the system's electromagnetic torque can achieve transient and rapid compensation, the position drop amplitude is significantly compressed and recovers very quickly, demonstrating excellent dynamic stiffness and disturbance resistance robustness. The comprehensive simulation data shows that the control strategy proposed in this paper fully achieves the expected design goals and has important theoretical significance and application reference value.

6. References

- [1] Cai S. Performance Analysis and Structural Optimization of Synchronous Reluctance Motor [D]. Zhejiang University, 2017.
- [2] Richalet J, Rault A, Testud J D, Papon J. Model predictive heuristic control: Applications to industrial processes[J]. Automatica, 1978, 14(5): 413–428.
- [3] Cutler C R, Ramaker B L. Dynamic matrix control — A computer control algorithm[C]// Proceedings of the Joint Automatic Control Conference. San Francisco, USA, 1980.
- [4] Clarke D W, Mohtadi C, Tuffs P S. Generalized predictive control — Part I: The basic algorithm[J]. Automatica, 1987, 23(2): 137–148.
- [5] Camacho E F, Bordons C. Model Predictive Control, 2nd ed. London: Springer, 2007.
- [6] Ogata K. Modern Control Engineering, 5th ed. Upper Saddle River, NJ: Prentice Hall, 2010.
- [7] Wang Y Z, et al. Dynamic modeling and control of PMSM position servo system[J]. Electronic Measurement Technology, 2024.
- [8] Zheng J, Peng C X, Yao C, et al. Low common-mode SVPWM method for PMSM vector control systems[J]. Manufacturing Automation, 2024, 46(12): 107–114.
- [9] Yu C, Kang E L. Fuzzy sliding mode sensorless control of permanent magnet synchronous motors[J]. Journal of Electrical Machines and Control, 2024, 28(1): 87–94.
- [10] Ma L H. Vector Control and SVPWM Algorithm Research of Dual Three-Phase PMSM [D]. Xihua University, 2023.
- [11] Sun P. Optimization of Current Loop in PMSM Vector Control System [D]. Qingdao University, 2020.
- [12] Bai A W. Research on Sensorless Control Technology of High-Speed PMSM [D]. Changchun University of Technology, 2020.
- [13] Guang K Y. Model Predictive Current Control of PMSM [D]. Dalian Jiaotong University, 2020.
- [14] Guo X, Zong J, Jiang H. Robust dual-vector model predictive current control of PMSM[J]. Modular Machine Tool & Automatic Manufacturing Technique, 2023(10): 91–99.
- [15] Li G. Application and analysis of vector control in electric vehicle drive systems[J]. Automotive Electric Appliances, 2024(9): 50–52.
- [16] Wu Q. Design and Implementation of PMSM Vector Control System [D]. Xi'an University of Technology, 2018.
- [17] Wen X, et al. Position control of DC motor based on sliding mode and high-gain observer[J]. Journal of University of Science and Technology of China, 2018.
- [18] Kong D Q, et al. Robust trajectory tracking control of parallel mechanism considering AC servo motor dynamics[J]. Acta Automatica Sinica, 2007.
- [19] Wei Q, et al. Friction compensation control of pneumatic position servo system with adjustable stiffness[J]. Journal of Northwestern Polytechnical University, 2024.
- [20] Luo B, et al. Visual servo tracking control for mobile robots based on adaptive dynamic programming[J]. Acta Automatica Sinica, 2023.
- [21] Tuyen T T, Yang J, Liao L, et al. Integrated sliding mode control for PMSM drives based on disturbance observer[J]. Electronics, 2025, 14(7): 1466.
- [22] Yan W C, Zhou L X, Liu D L. Research and application of PMSM AC servo system[J]. Electric Machines & Control Application, 2010, 37(5): 49–51.
- [23] Afzal H, Mufti M R, Din S U, et al. Modeling and inverse complex generalized synchronization and parameter identification of nonlinear systems using adaptive integral sliding mode control[J]. IEEE Access, 2020, 8: 38950–38969.
- [24] Zhou W L. Research on Parameter Identification Methods of PMSM [D]. Shandong University, 2023.
- [25] He W. Servo Control Strategy of Dual-Axis Pointing Mechanism for Spaceborne Antenna [D]. Southwest University of Science and Technology, 2023.
- [26] Qu Y P. Performance Improvement of PMSM Speed Control Based on Load State Estimation and Compensation [D]. Harbin Institute of Technology, 2014.
- [27] Liu J, Yang P, Ma W L, et al. Simulation of PMSM sliding mode control algorithm based on fuzzy switching gain regulation[J]. Electronic Measurement Technology, 2019, 42(19): 106–110.

- [28] Chen X, Zheng S L, Hou Y, et al. Active vibration suppression of electric vehicle transmission system using sliding mode control[J]. *Machine Design and Manufacturing*, 2024(3): 218–223.
- [29] Sun Z Y, Xu S, Ren G Z, et al. Dual-mode model predictive control strategy for full-speed range PMSM traction motors[J]. *Proceedings of the CSEE*, 2025, 45(2): 748–758.
- [30] Yuan Q Q, Qiu H F. Improved sliding mode disturbance observer for induction motor control system[J]. *Electronic Science*, 2022, 35(2): 59–66.
- [31] Yang J F, Zhang Y F, Cao W, et al. Analysis of torque-flux coupling characteristics of brushless DC motors[J]. *Journal of Electrical Machines and Control*, 2019, 23(10): 95–101.
- [32] Yang Y, Han J G, Chen H, et al. Research on model predictive control of PMSM[J]. *Journal of Power Supply*, 2015, 13(4): 58–63.
- [33] Lan Z Y, Wang B, Xu C, et al. A novel three-vector model predictive current control for PMSM[J]. *Proceedings of the CSEE*, 2018, 38(S1): 243–249.
- [34] Zhu R, Wu D, Chen J F, et al. Review of model predictive control for motor systems[J]. *Electric Machines & Control Application*, 2019, 46(8): 1–10, 30.
- [35] Qiu J Q, Mao Y H, Chen Z Y, et al. Finite control set model predictive speed control for PMSM[J]. *Journal of Electrical Machines and Control*, 2023, 27(4): 1–9.
- [36] Chen R, Zhai K M, Shu H P. Dual-vector fixed switching frequency model predictive control of PMSM[J]. *Transactions of China Electrotechnical Society*, 2023, 38(14): 3812–3823.
- [37] Yi B Y, Kang L Y, Feng C Z, et al. Disturbance observer-based predictive current control for PMSM[J]. *Transactions of China Electrotechnical Society*, 2016, 31(18): 37–45.
- [38] Yang X W, Niu M J, Li H, et al. Improved model predictive control based on switching-state function computation[J]. *Transactions of China Electrotechnical Society*, 2018, 33(20): 4834–4844.
- [39] Xu Y P, Zhang B C, Zhou Q. Dual-vector model predictive current control for PMSM[J]. *Transactions of China Electrotechnical Society*, 2017, 32(20): 222–230.
- [40] Zhang Y F, Wu Z H, Yan Q, et al. Parameter-free three-vector model predictive current control for PMSM[J]. *Journal of Northwestern Polytechnical University*, 2023, 41(5): 860–870.